Chinese Journal of Structural Chemistry

ARTICLE

Hollow Fe_4C/FeP Nanoboxes with Heterostructure and Carbon Armor for Efficient and Stable Hydrogen Evolution

Jing-Yi Xie[1], Hui-Ying Zhao[1], Yi-Wen Dong[1], Yang Wu[1], Da-Peng Liu[1]*, Yong-Ming Chai[1] and Bin Dong[1]*

[1]*State Key Laboratory of Heavy Oil Processing, College of Chemistry and Chemical Engineering, China University of Petroleum (East China), Qingdao 266580, China*

ABSTRACT The heterojunction interfacial modulation of FeP is an effective strategy to regulate the intrinsic activity and stability, which is a major challenge to promote the industrial application of FeP-based electrocatalysts. Herein, hollow Fe_4C/FeP box with heterojunction interface and carbon armor is successfully synthesized, which can expose numerous active sites and protect catalyst from corrosion. Electrochemical measurements show that Fe_4C/FeP exhibits excellent hydrogen evolution activity and stability. It only needs 180 mV to achieve the current density of 10 mA cm^{-2}. The high-activity may be due to the synergistic effects of porous framework, graphitic carbon coating and heterojunction structure of Fe_4C and FeP, which optimize the electronic structure and accelerates electron transfer. In addition, the target catalyst can withstand 5000 cycles of CV testing without significant change in properties. The excellent stability may be attributed to the graphitic carbon coating as the armor that can prevent the catalyst from corrosion of electrolyte. This work may provide a synthetic approach to produce a series of carbon-coated and heterojunction structure of transition metal phosphides for water splitting.

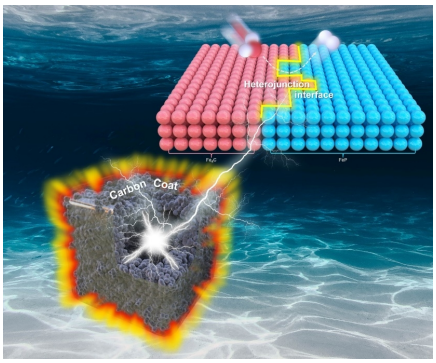

Keywords: carbon armor, hollow box, heterostructured electrocatalysts, hydrogen evolution reaction

n INTRODUCTION

Molecular hydrogen (H_2) is considered as a green and sustainable feedstock with high energy density for hydrogen economy in the future.[1-6] Currently, electrochemical water splitting driven by renewable energy is a promising method to generate H_2.[7,8] Because of the superior activity and stability, platinum (Pt)-based catalysts are the main choice for commercial.[9-11] However, largescale H_2 production is limited by the scarcity and high price of Pt-group precious metals.[12-14] To address this issue, efficient and low-cost electrocatalysts are highly imperative to design and develop for hydrogen production.[15-18]

Iron is currently one of the most abundant and cheapest transition metals. Thus, considerable efforts have been put into the exploration of Fe-based electrocatalyst, such as sulfides,[19,20] phosphides,[21-25] and carbides,[26-28] for hydrogen production. Among these catalysts, as a promising HER catalyst, the property of pure FeP is unsatisfactory. Interestingly, the fascinating synergistic effects derived from the heterojunction interface of the combination of different types of materials can provide multiple functional sites during hydrogen evolution reaction.[29] Thus, the heterostructured catalysts are a promising choice to design catalyst with high performance and even new functionality.[30] For example, Niu et al. have synthesized the hierarchical CoP-FeP branched heterostructures which exhibit remarkable electrocatalytic performance towards HER under acidic conditions and a 30 mV performance improvement over pure FeP.[31] However, most of the reported heterojunction structures are bimetallic or trimetallic heterojunctions.[32] The structures of iron-based heterojunctions without the introduction of second-class metals are rarely reported and are full of challenging.

Herein, we propose an effective method to synthesize Fe_4C/FeP heterostructured catalysts with hollow box structure and carbon coat using Prussian blue (PB) as the precursor, which exhibits excellent hydrogen evolution activity and stability. The in-situ carbonization of organic ligands forms the outside carbon layer as armor, which can prevent them from the destruction of acidic electrolyte. During the hydrogen evolution reaction (HER), Fe_4C/FeP exhibits remarkable catalytic activity superior to pure FeP, with a Tafel slope of 70.7 mV dec^{-1} and an overpotential of 180 mV to achieve 10 mA cm^{-2}. Besides, the target catalyst shows no significant degradation after 5000 cycles of CV testing, indicating excellent durability of the catalyst.

n RESULTS AND DISCUSSION

As illustrated in Scheme 1, Fe_4C/FeP possesses a cubic framework with cavity and carbon armor, which was synthesized via a two-step method, including the calcination of Prussian Blue (PB) precursor in air and the following phosphating process. In order to reveal the crystalline phase structure, Fe_4C/FeP, Fe_3C and PB were characterized by X-ray diffraction (XRD). As shown in Figure 1a, PB (PDF No. 01-073-0689) is calcined to form Fe_3C (PDF No. 01-077-0255), which is reduced to Fe_4C after phosphating. Besides, the XRD pattern of Fe_4C/FeP suggests the formation of FeP (PDF No. 01-078-1443) and Fe_4C (PDF No. 01-089-4053). Concretely, the diffraction peaks of Fe_4C/FeP approximated at 30.851°, 32.748°, 48.315° and 56.078° belong to (002), (011), (211) and (212) crystallographic planes of FeP. Also, the peaks at 40.247°, 46.815°, 68.363° and 82.416° are well-consistent with (111), (200), (220) and (311) crystal planes of Fe_4C, implying the coexistence of FeP and Fe_4C formed on Fe_4C/FeP.

The X-ray photoelectron spectroscopy (XPS) is employed to in-

DOI: 10.14102/j.cnki.0254-5861.2022-0102

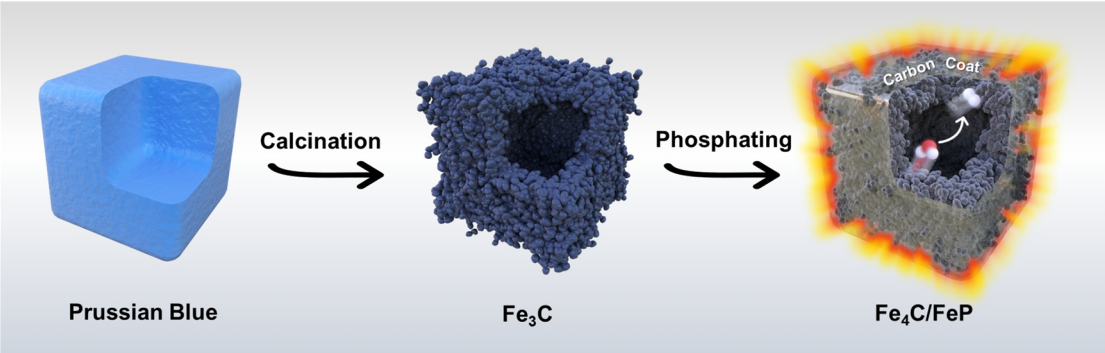

Scheme 1. Schematic illustration of the preparation of Fe_4C/FeP.

vestigate the chemical composition and the change in electronic states of Fe_4C/FeP. As depicted in Figure S1, the characteristic peaks of Fe, P, C and O can be observed. As for Fe 2p in Fe_4C/FeP (Figure 1b), the peak has been divided in two couples of Fe $2p_{3/2}$ and Fe $2p_{1/2}$. The binding energies at 707.2 and 720.2 eV are corresponding to the Fe-P species.[33,34] Besides, the peaks at 710.4 and 724.3 eV belong to Fe-O bonds.[35] Notably, a negative shift can be observed in the Fe-P of Fe_4C/FeP, indicating that the electron structure of FeP has redistributed. In addition, the P 2p peaks (Figure 1c) from Fe_4C/FeP have two couples of P $2p_{3/2}$ and P $2p_{1/2}$, which indicates the formation of bond between Fe and P. Another peak at around 133.5 eV belongs to phosphate formed by surface oxidation.[36,37] It also exhibits negative shift in Fe_4C/FeP relative to that of FeP. This phenomenon can be attributed to the improved electron transfer between Fe and P. The peak at 285 eV in C 1s spectrum of Fe_4C/FeP (Figure S2) is attributed to graphitic carbon, C-C or C=C.[38,39] It is noted that peak intensity of graphitic carbon is strong, which is essential to the improvement of conductivity and stability of Fe_4C/FeP.[40]

The morphologic and structural characteristics of Fe_4C/FeP and other contrast samples are investigated by scanning electron microscope (SEM) and high-resolution transmission electron microscopy (HRTEM). SEM images in Figure 2a and b show that Prussian blue as the precursor has a uniform and evenly distributed nanocube structure. After calcination in air, the surface of Fe_3C (Figure 2c-d) becomes rougher. As shown in Figure 2e-f, the overall morphology of Fe_4C/FeP remains largely unchanged after phosphating, in which the rough and porous surface can provide numerous active sites to enhance its electrocatalytic activity. As a comparison, the surface of FeP obtained by direct phosphating of the precursor Prussian blue (Figure S3) is smoother than that of Fe_3C and Fe_4C/FeP, which may reduce the exposure of active sites.

The inside hollow structure of Fe_4C/FeP is verified by TEM images. As shown in Figure 3a, PB as a precursor has a solid cubic structure with the size of around 206 nm, which is highly dispersed and uniform in size (Figure S4), while after calcination and phosphating, the Fe_4C/FeP possesses a large cavity inside (Figure 3b). In addition, there is a uniformly dispersed and completely wrapped carbon layer on the outer surface of the catalyst (Figure 3c), and the thickness of the carbon layer is about 6 nm which can be obtained from the insert figure. It is speculated that the carbon layer is obtained by carbonization of cyanide groups uniformly dispersed in the PB structure, which acts as the armor to prevent corrosion and also enhance the conductivity of catalyst. To further explore the detailed structural information of Fe_4C/FeP, HRTEM image is exhibited in Figure 3d, in which the distinct lattice fringes of 0.193 and 0.288 nm can be found corresponding to the (200)

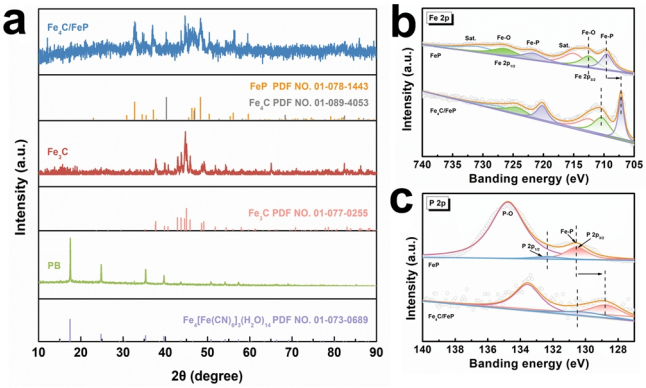

Figure 1. (a) XRD of PB, Fe_3C and Fe_4C/FeP. (b, c) XPS of Fe 2p and P 2p in FeP and Fe_4C/FeP.

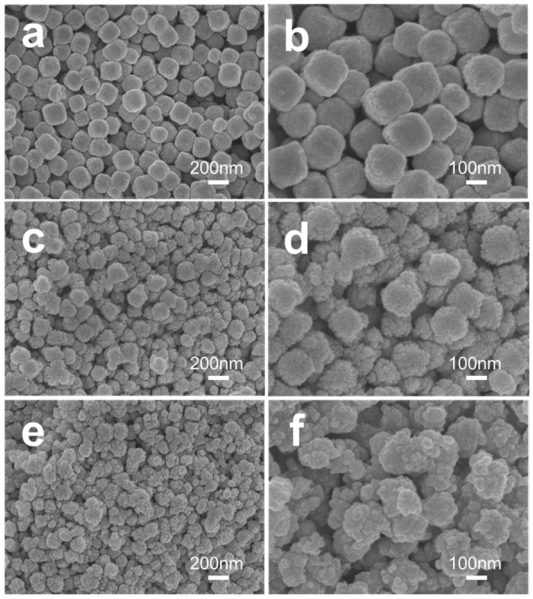

Figure 2. SEM images of (a, b) PB, (c, d) Fe_3C and (e, f) Fe_4C/FeP.

Chin. J. Struct. Chem. **2022**, 41, 2207053-2207058
DOI: 10.14102/j.cnki.0254-5861.2022-0102

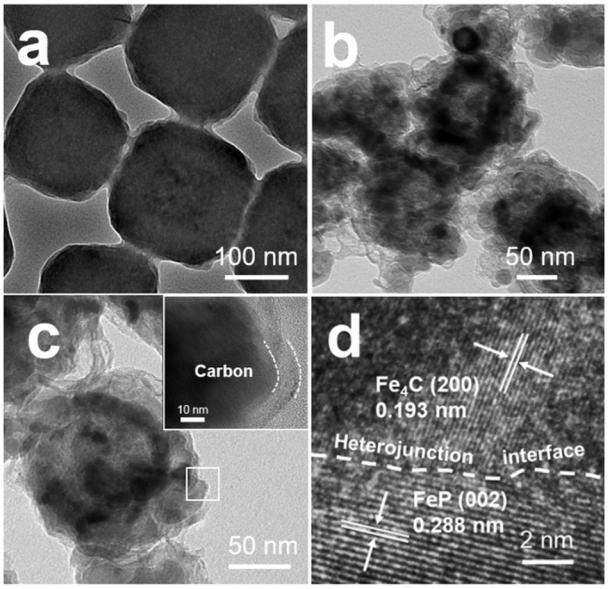

Figure 3. (a) TEM image of PB. (b, c) TEM images and (d) HRTEM image of Fe_4C/FeP.

crystal plane of Fe_4C and (002) crystal plane of FeP, respectively. Besides, there is a distinct heterojunction interface between Fe_4C and FeP. This result is consistent with the conclusion from XRD and XPS. In addition, there is a distinct heterojunction interface between Fe_4C and FeP, which can induce electron redistribution at the interface. This is beneficial to the surface electron modulation of the heterostructure and enhances the intrinsic catalytic activity.[32] Figure S5 and S6 are the TEM images of Fe_3C and FeP with partial hollow cavity. It is speculated that cyano group in PB will gradually decompose when the temperature rises,[41] and the calcination temperature is the key point to control the formation of Fe_4C/FeP box with hollow structure.

As illustrated in Figure 4a and b, linear scan voltammetry (LSV) curve of Fe_4C/FeP is measured with a scan rate of 5 mV s^{-1} on the reversible hydrogen electrode (RHE) scale. As contrast samples, Pt/C, GCE, PB, FeP and Fe_3C are also characterized for comparison. The tested potentials are converted to reversible hydrogen electrode (RHE), calculated by the Nernst equation. Fe_4C/FeP exhibits excellent electrocatalytic activity, and only needs 180 mV to achieve 10 mA cm^{-2}, which is much lower than that of other samples. By contrast, FeP needs 340 mV to reach 10 mA cm^{-2}. This phenomenon may be due to the heterojunction structure formed by Fe_4C and FeP, benefiting from the heterojunction interface with high catalytic activity. Besides, Fe_4C/FeP electrode has lower overpotential than many active HER catalysts under acidic media (Table S1). As illustrated in Figure 4c, Fe_4C/FeP shows a low Tafel slope (70.7 mV dec^{-1}) which follows the mechanism of Volmer-Heyrovsky, where the adsorbed hydrogen atom prefers to couple with another proton in the electrolyte and a new electron to evolve H_2.[42] And the Tafel slopes of other contrast samples including Fe_3C (111.8 mV dec^{-1}), FeP (122.2 mV dec^{-1}), PB (669.9 mV dec^{-1}) and Pt/C (37 mV dec^{-1}) are also demonstrated. In order to further prove the conductivity of Fe_4C/FeP, the analysis of electrochemical impedance spectroscopy is carried out by Nyquist plots in high-frequency semicircle region at the voltage of -0.35 V vs. RHE, as shown in Figure 4d. Fe_4C/FeP (351 Ω) shows the smallest semicircle in the Nyquist plots compared with PB (7.2 GΩ), FeP (1807 Ω) and Fe_3C (9.1 GΩ), suggesting the existence of carbon layer enhanced the conductivity of target catalyst and accelerated the charge transfer. As shown in Figure 4e, the double-layer capacitance (C_{dl}) of Fe_4C/FeP is estimated to be 0.564 mF cm^{-2}, which is superior to that of other contrastive samples, suggesting more active sites can be exposed due to the porous structure and heterojunction interfaces between Fe_4C and FeP.

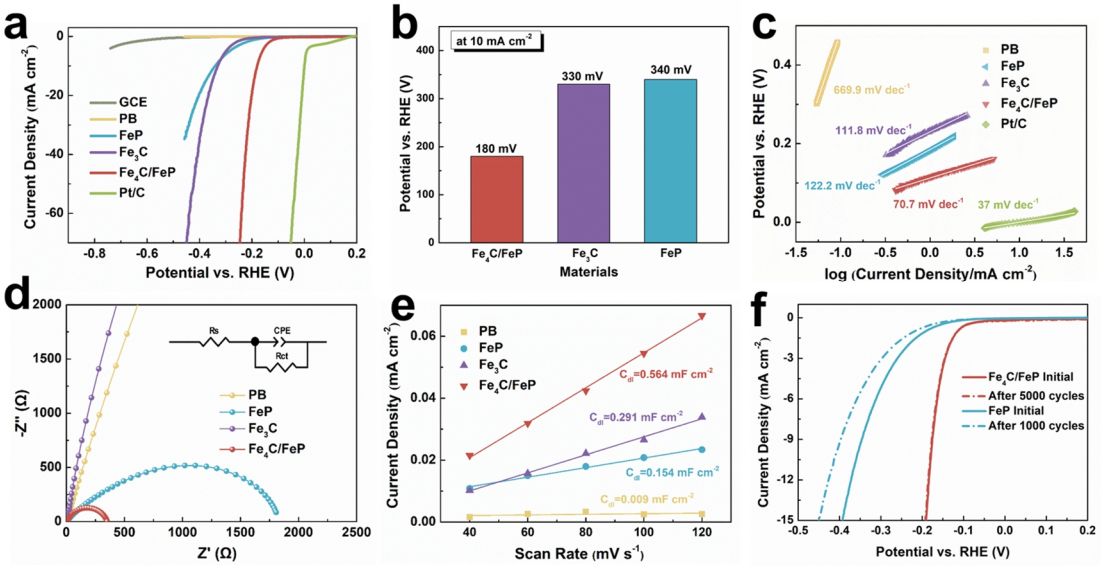

Figure 4. HER performance of Fe_4C/FeP and other contrast samples in 0.5 M H_2SO_4. (a) LSV curves, (b) Comparison of overpotentials at 10 mA cm^{-2}, (c) Tafel plots, (d) Nyquist plots, (e) Double-layer capacitances, (f) LSV curves of Fe_4C/FeP and FeP before and after thousands of CV cycles at a scan rate of 100 mV s^{-1}.

DOI: 10.14102/j.cnki.0254-5861.2022-0102

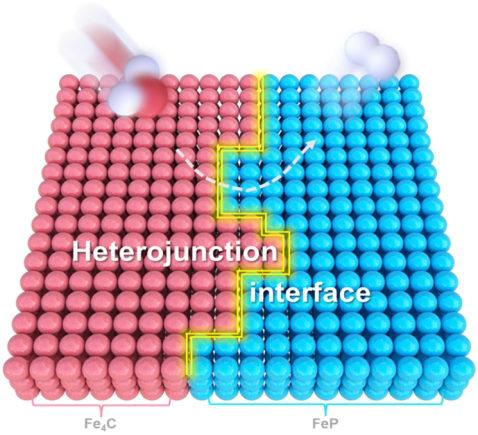

Figure 5. Schematic diagram of the heterojunction interface function between Fe_4C and FeP in Fe_4C/FeP.

Furthermore, to evaluate the long-term stability of Fe_4C/FeP, 5000 cycles of continuous CV test at a scan rate of 100 mV s^{-1} is carried out in acid solution (Figure 4f). Obviously, LSV of Fe_4C/FeP after 5000 cycles CV test shows no significant change. On the contrast, FeP alone shows noticeable decay after only 1000 cycles. The excellent durability of Fe_4C/FeP may be attributed to the optimized electron density of both Fe_4C and FeP, and formed highly active heterojunction interfaces. Besides, carbon layer formed during high temperature calcination plays an important role in both high activity and durability. On one hand, the existence of graphitic carbon coating can enhance the conductivity of target catalyst and accelerates the charge transfer. On the other hand, the armor can also prevent the catalyst from corrosion of electrolyte, which contributed to the excellent stability of Fe_4C/FeP. Meanwhile, chronoamperometry measurement is also carried out (Figure S7). The current density (20 mA cm^{-2}) of Fe_4C/FeP maintains nearly invariable during 15 h test under a constant voltage of -0.37 V (vs. RHE) for hydrogen evolution reaction.

Combined with the above experimental conclusions, the superior catalytic activity of Fe_4C/FeP could be attributed to the synergistic effects of porous structure, carbon coating and heterojunction interface function between Fe_4C and FeP (Figure 5). Specifically, the porous structure can promote the contact between the active sites and the electrolyte, which is conducive to the progress of the catalytic reaction. In addition, the formation of carbon layer after carbonization at high temperature can decrease the contact electrical resistance and lead to fast electron transportation, which further improves the hydrogen production rate.[43,44] Moreover, the heterojunction structure of Fe_4C and FeP can accelerate electron transfer between Fe and P, thus improving their electronic structures to help the catalyst for highly active electrolysis of water for hydrogen production. Finally, carbon layer as armor can enhance the stability of the Fe_4C/FeP in acidic electrolyte.

n CONCLUSIONS

In summary, the hollow Fe_4C/FeP box with heterojunction interface and carbon armor is successfully synthesized via a two-step method, including the calcination in air and the following phosphating. The Fe_4C/FeP which derives from PB ($Fe_4[Fe(CN)_6]_3$) exhibits excellent hydrogen evolution activity. The enhanced catalytic activity can be ascribed to the porous structure, graphitic carbon armor and heterojunction interface function between Fe_4C and FeP, which optimizes the electronic structure and accelerates electron transfer. The long-term stability can be attributed to the carbon layer as armor to prevent it from corrosion in acidic solution. This work may provide a synthetic approach to produce a series of carbon-coated and heterojunction structure of transition metal phosphides for water electrolysis.

n EXPERIMENTAL

To prepare PB, 0.01 mol $K_4[Fe(CN)_6]$ was added into 40 mL HCl (0.1 M) within 3 g PVP under stirring. Then the solution was reacted at 80 ℃ for 12 h. After centrifugation and washing, PB was collected.

Subsequently, 0.1 g PB was calcined under argon atmosphere for 2 h at 700 ℃ with a temperature ramp of 2 ℃ min^{-1}. The obtained samples were marked as Fe_3C.

0.01 g Fe_3C and 0.2 g $NaH_2PO_2 \cdot H_2O$ were placed in a tube furnace with two separate porcelain boats under argon atmosphere for 2 h at 350 ℃. After the apparatus was cooled to room temperature, products were obtained which are denoted as Fe_4C/FeP. The materials, physical characterization and electrochemical measurements can be found in the supplementary material.

n ACKNOWLEDGEMENTS

This work is financially supported by National Natural Science Foundation of China (52174283) and Innovation Fund Project for Graduate Students of China University of Petroleum (East China) (No. CXJJ-2022-23).

n AUTHOR INFORMATION

Corresponding authors. Emails: liudp@upc.edu.cn (D. Liu) and dongbin@upc.edu.cn (B. Dong)
Tel: +86-532-86981156, Fax: +86-532-86981156

n COMPETING INTERESTS

The authors declare no competing interests.

n ADDITIONAL INFORMATION

Supplementary information is available for this paper at http://manu30.magtech.com.cn/jghx/EN/10.14102/j.cnki.0254-5861.2022-0102

For submission: https://mc03.manuscriptcentral.com/cjsc

n REFERENCES

(1) Guo, K.; Wang, Y.; Huang, J.; Lu, M.; Li, H.; Peng, Y.; Xi, P.; Zhang, H.; Huang, J.; Lu, S.; Xu, C. In situ activated $Co_{3-x}Ni_xO_4$ as a highly active and ultrastable electrocatalyst for hydrogen generation. *ACS Catal.* **2021**, 11, 8174-8182.

(2) Liu, Z.; Zhang, C.; Liu, H.; Feng, L. Efficient synergism of $NiSe_2$ nanoparticle/NiO nanosheet for energy-relevant water and urea electrocatalysis. *Appl. Catal. B* **2020**, 276, 119165.

(3) Liu, Z.; Yu, X.; Xue, H.; Feng, L. A nitrogen-doped CoP nanoarray over 3D porous Co foam as an efficient bifunctional electrocatalyst for

DOI: 10.14102/j.cnki.0254-5861.2022-0102

overall water splitting. *J. Mater. Chem. A* **2019**, 7, 13242-13248.
(4) Zhu, Y. G.; Shang, C. Q.; Wang, Z. Y.; Zhang, J. Q.; Yang, M. Y.; Cheng, H.; Lu, Z. G. Co and N co-modified carbon nanotubes as efficient electrocatalyst for oxygen reduction reaction. *Rare Met.* **2021**, 40, 90-95.
(5) Wang, Y.; Huang, J.; Wang, L.; She, H.; Wang, Q. Research progress of ferrite materials for photoelectrochemical water splitting. *Chin. J. Struct. Chem.* **2022**, 41, 2201054-2201068.
(6) Yan, T.; Zhang, X.; Liu, H., Jin, Z. CeO_2 particles anchored to Ni_2P nanoplate for efficient photocatalytic hydrogen evolution. *Chin. J. Struct. Chem.* **2022**, 41, 2201047-2201053.
(7) Zhang, C.; Tang, B.; Gu, X.; Feng, L. Surface chemical state evaluation of $CoSe_2$ catalysts for the oxygen evolution reaction. *Chem. Commun.* **2019**, 55, 10928-10931.
(8) Li, M.; Feng, L. $NiSe_2$-CoS_2 with a hybrid nanorods and nanoparticles structure for efficient oxygen evolution reaction. *Chin. J. Struct. Chem.* **2022**, 41, 2201019-2201024.
(9) Dong, B.; Xie, J. Y.; Wang, N.; Gao, W. K.; Ma, Y.; Chen, T. S.; Yan, X. T.; Li, Q. Z.; Zhou, Y. L.; Chai, Y. M. Zinc ion induced three-dimensional Co_9S_8 nano-neuron network for efficient hydrogen evolution. *Renew. Energy* **2020**, 157, 415-423.
(10) Niu, C.; Zhang, Y.; Dong, J.; Yuan, R.; Kou, W.; Xu, L. 3D ordered macro-/mesoporous NixCo100-x alloys as high-performance bifunctional electrocatalysts for overall water splitting. *Chin. Chem. Lett*. **2021**, 32, 2484-2488.
(11) Zhang, C.; Cui, Y.; Yang, Y.; Lu, L.; Yu, S.; Meng, Z.; Wu, Y.; Li, Y.; Wang, Y.; Tian, H.; Zheng, W. Highly conductive amorphous pentlandite anchored with ultrafine platinum nanoparticles for efficient pH-universal hydrogen evolution reaction. *Adv. Funct. Mater.* **2021**, 31, 2105372.
(12) Yang, Y.; Yu, Y.; Li, J.; Chen, Q.; Du, Y.; Rao, P.; Li, R.; Jia, C.; Kang, Z.; Deng, P.; Shen, Y.; Tian, X. Engineering ruthenium-based electrocatalysts for effective hydrogen evolution reaction. *Nano-Micro Lett*. **2021**, 13, 160.
(13) Wang, Y. H.; Li, R. Q.; Li, H. B.; Huang, H. L.; Guo, Z. J.; Chen, H. Y.; Zheng, Y.; Qu, K. G. Controlled synthesis of ultrasmall RuP_2 particles on N,P-codoped carbon as superior pH-wide electrocatalyst for hydrogen evolution. *Rare Met.* **2021**, 40, 1040-1047.
(14) Li, P.; Hong, W.; Liu, W. Fabrication of large scale self-supported WC/$Ni(OH)_2$ electrode for high-current-density hydrogen evolution. *Chin. J. Struct. Chem.* **2021**, 40, 1365-1371.
(15) Guo, B. Y.; Zhang, X. Y.; Ma, X.; Chen, T. S.; Chen, Y.; Wen, M. L.; Qin, J. F.; Nan, J.; Chai, Y. M.; Dong, B. RuO_2/Co_3O_4 Nanocubes based on Ru ions impregnation into prussian blue precursor for oxygen evolution. *Inter. J. Hydrogen Energy* **2020**, 45, 9575-9582.
(16) Li, X. P.; Huang, C.; Han, W. K.; Ouyang, T.; Liu, Z. Q. Transition metal-based electrocatalysts for overall water splitting. *Chin. Chem. Lett*. **2021**, 32, 2597-2616.
(17) Wang, X.; He, Y.; Han, X.; Zhao, J.; Li, L.; Zhang, J.; Zhong, C.; Deng, Y.; Hu, W. Engineering cobalt sulfide/oxide heterostructure with atomically mixed interfaces for synergistic electrocatalytic water splitting. *Nano Res.* **2022**, 15, 1246-1253.
(18) Fu, C.; Wang, Y., Huang, J. Hybrid of quaternary layered double hydroxides and carbon nanotubes for oxygen evolution reaction. *Chin. J. Struct. Chem.* **2020**, 39, 1807-1816.
(19) Zhou, G.; Shan, Y.; Wang, L.; Hu, Y.; Guo, J.; Hu, F.; Shen, J.; Gu, Y.; Cui, J.; Liu, L., Wu, X. Photoinduced semiconductor-metal transition in ultrathin troilite FeS nanosheets to trigger efficient hydrogen evolution. *Nat. Commun.* **2019**, 10, 399.
(20) Wang, L.; Shan, Y.; Liu, L. Enhancing hydrogen evolution reaction by strain engineering in free-standing doped FeS monolayer. *Mater. Chem. Phys.* **2020**, 239, 122046.
(21) Pei, H.; Zhang, L.; Zhi, G.; Kong, D.; Wang, Y.; Huang, S.; Zang, J.; Xu, T.; Wang, H.; Li, X. Rational construction of hierarchical porous FeP nanorod arrays encapsulated in polypyrrole for efficient and durable hydrogen evolution reaction. *Chem. Eng. J.* **2022**, 433, 133643.
(22) Wu, Y.; Wang, Y.; Wang, Z.; Li, X. Highly dispersed CoP on three-dimensional ordered mesoporous FeP for efficient electrocatalytic hydrogen production. *J. Mater. Chem. A* **2021**, 9, 23574-23581.
(23) Von Lim, Y.; Huang, S.; Zhang, Y.; Kong, D.; Wang, Y.; Guo, L.; Zhang, J.; Shi, Y.; Chen, T. P.; Ang, L. K.; Yang, H. Y. Bifunctional porous iron phosphide/carbon nanostructure enabled high-performance sodium-ion battery and hydrogen evolution reaction. *Energy Stor. Mater.* **2018**, 15, 98-107.
(24) Xu, Y.; Li, N.; Wang, R.; Xu, L.; Liu, Z.; Jiao, T.; Liu, Z. Self-assembled FeP/MoP co-doped nanoporous carbon matrix for hydrogen evolution application. *Colloids Surfaces A* **2022**, 636, 128206.
(25) Son, C. Y.; Kwak, I. H.; Lim, Y. R.; Park, J. FeP and FeP_2 nanowires for efficient electrocatalytic hydrogen evolution reaction. *ChemComm* **2016**, 52, 2819-2822.
(26) Lin, H.; Zhang, W.; Shi, Z.; Che, M.; Yu, X.; Tang, Y.; Gao, Q. Electrospinning hetero-nanofibers of Fe_3C-Mo_2C/nitrogen-doped-carbon as efficient electrocatalysts for hydrogen evolution. *ChemSusChem* **2017**, 10, 2597-2604.
(27) Yang, C. C.; Zai, S. F.; Zhou, Y. T.; Du, L.; Jiang, Q. Fe_3C-Co nanoparticles encapsulated in a hierarchical structure of N-doped carbon as a multifunctional electrocatalyst for ORR, OER, and HER. *Adv. Funct. Mater.* **2019**, 29, 1901949.
(28) Gao, S.; Chen, H.; Liu, Y.; Gao, R.; Li, G. D.; Zou, X. Surface-clean, phase-pure multi-metallic carbides for efficient electrocatalytic hydrogen evolution reaction. *Inorg. Chem. Frontiers* **2019**, 6, 940-947.
(29) Wei, J.; Zhou, M.; Long, A.; Xue, Y.; Liao, H.; Wei, C.; Xu, Z. J. Heterostructured electrocatalysts for hydrogen evolution reaction under alkaline conditions. *Nanomicro. Lett.* **2018**, 10, 75.
(30) Hu, W.; Shi, Q.; Chen, Z.; Yin, H.; Zhong, H.; Wang, P. Co_2N/$Co_2Mo_3O_8$ heterostructure as a highly active electrocatalyst for an alkaline hydrogen evolution reaction. *ACS Appl. Mater. Interfaces* **2021**, 13, 8337-8343.
(31) Niu, Z.; Qiu, C.; Jiang, J.; Ai, L. Hierarchical CoP-FeP branched heterostructures for highly efficient electrocatalytic water splitting. *ACS Sustain. Chem. Eng.* **2019**, 7, 2335-2342.
(32) Su, J.; Li, G. D.; Li, X. H.; Chen, J. S. 2D/2D heterojunctions for catalysis. *Adv. Sci.* **2019**, 6, 1801702.
(33) Wang, M.; Tuo, Y.; Li, X.; Hua, Q.; Du, F.; Jiang, L. Mesoporous Mn-doped FeP: facile synthesis and enhanced electrocatalytic activity for hydrogen evolution in a wide pH range. *ACS Sustain. Chem. Eng.* **2019**, 7, 12419-12427.
(34) Qian, C.; Kim, F.; Ma, L.; Tsui, F.; Yang, P.; Liu, J. Solution-phase synthesis of single-crystalline iron phosphide nanorods/nanowires. *J. Am. Chem. Soc.* **2004**, 126, 1195-1198.
(35) Zhang, X.; Li, F.; Shi, Z.; Dong, B.; Dong, Y.; Wu, Z.; Wang, L.; Liu, C.; Chai, Y. Vanadium doped FeP nanoflower with optimized electronic structure for efficient hydrogen evolution. *J. Colloid Interface Sci.* **2022**, 615, 445-455.

DOI: 10.14102/j.cnki.0254-5861.2022-0102

(36) Luo, Y.; Qiu, W.; Liang, R.; Xia, X.; Qiu, J. Mo-doped FeP nanospheres for artificial nitrogen fixation. *ACS Appl. Mater. Interfaces* **2020**, 12, 17452-17458.

(37) Feng, L.; Zhang, X.; Huang, J.; He, D.; Li, X.; Liu, Q.; Feng, Y.; Li, G.; Xu, G.; Cao, L. Fe_2P encapsulated in carbon nanowalls decorated with well-dispersed Fe_3C nanodots for efficient hydrogen evolution and oxygen reduction reactions. *Nanoscale* **2021**, 13, 17920-17928.

(38) Liu, W.; Liu, G.; Shi, N.; Liu, D.; Wen, F. Carbon quantum dot-modified and chloride-doped ordered macroporous graphitic carbon nitride composites for hydrogen evolution. *ACS Appl. Nano Mater.* **2020**, 3, 12188-12197.

(39) Zhu, X.; Zhao, T.; Nie, Z.; Liu, Y.; Yao, S. Non-redox modulated fluorescence strategy for sensitive and selective ascorbic acid detection with highly photoluminescent nitrogen-doped carbon nanoparticles via solid-state synthesis. *Anal. Chem.* **2015**, 87, 8524-8530.

(40) Zhu, X.; Liu, M.; Liu, Y.; Chen, R.; Nie, Z.; Li, J.; Yao, S. Carbon-coated hollow mesoporous FeP microcubes: an efficient and stable electrocatalyst for hydrogen evolution. *J. Mater. Chem. A* **2016**, 4, 8974-8977.

(41) Zhang, G.; Li, Y.; Xiao, X.; Shan, Y.; Bai, Y.; Xue, H. G.; Pang, H.; Tian, Z.; Xu, Q. In situ anchoring polymetallic phosphide nanoparticles within porous prussian blue analogue nanocages for boosting oxygen evolution catalysis. *Nano Lett.* **2021**, 21, 3016-3025.

(42) Shi, Y.; Zhang, B. Correction: recent advances in transition metal phosphide nanomaterials: synthesis and applications in hydrogen evolution reaction. *Chem. Soc. Rev.* **2016**, 45, 1781-1781.

(43) Deng, J.; Ren, P.; Deng, D.; Bao, X. Enhanced electron penetration through an ultrathin graphene layer for highly efficient catalysis of the hydrogen evolution reaction. *Angew. Chem. Int. Ed.* **2015**, 54, 2100-2104.

(44) Jiang, H.; Yan, L.; Zhang, S.; Zhao, Y.; Yang, X.; Wang, Y.; Shen, J.; Zhao, X.; Wang, L. Electrochemical surface restructuring of phosphorus-doped carbon@MoP electrocatalysts for hydrogen evolution. *Nano-Micro Lett*. **2021**, 13, 215.

Received: April 30, 2022
Accepted: May 18, 2022
Published online: May 23, 2022
Published: July 18, 2022

DOI: 10.14102/j.cnki.0254-5861.2022-0102